Science of the Total Environment 850 (2022) 158017

Contents lists available at ScienceDirect

Science of the Total Environment

journal homepage: www.elsevier.com/locate/scitotenv

Gene/environment interaction in the susceptibility of Crohn's disease patients to aluminum

Madjid Djouina [a], Christophe Waxin [a], Frédéric Leprêtre [b], Meryem Tardivel [b], Olivier Tillement [c], Francis Vasseur [d], Martin Figeac [b], Antonino Bongiovanni [b], Shéhérazade Sebda [b], Pierre Desreumaux [a], David Launay [a], Laurent Dubuquoy [a], Mathilde Body-Malapel [a], Cécile Vignal [a,*]

[a] Univ. Lille, Inserm, CHU Lille, U1286- INFINITE - Institute for translational research in inflammation, F-59000 Lille, France
[b] Univ. Lille, CNRS, Inserm, CHU Lille, Institut Pasteur de Lille, US 41 - UAR 2014 - PLBS, F-59000 Lille, France
[c] Institut Lumière Matière, Université Claude Bernard Lyon 1, CNRS UMR 5306, 69622 Villeurbanne, France
[d] Univ. Lille, CHU Lille, ULR 2694-METRICS : Évaluation des technologies de santé et des pratiques médicales, F-59000 Lille, France

HIGHLIGHTS

- Aluminum exposure induced inflammatory cytokine secretion in colon of Crohn's disease but not healthy patients.
- Aluminum internalisation in intestinal epithelial cells was correlated to inflammation.
- Patients bearing genetic polymorphism in MDR1 or SLC26A3 showed a higher susceptibility to aluminum-induced inflammation.

GRAPHICAL ABSTRACT

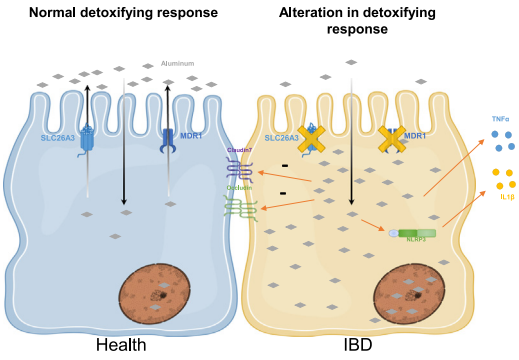

ARTICLE INFO

Editor: Katarzyna Kordas

Keywords:
Xenobiotics
Transporters
MDR1
SLC26A3
Polymorphisms

ABSTRACT

Background & aim: The key role of environmental factors in the pathogenesis of Inflammatory Bowel Diseases (IBD) is recognized. Aluminum is suspected to be a risk factor for IBD. However, mechanisms linking aluminum exposure to disease development are unknown. We examined the role of aluminum transport and subcellular localisation on human colon susceptibility to aluminum-induced inflammation.
Methods: Human colon biopsies isolated from Crohn's disease (CD) or control patients and Caco-2 cells were incubated with aluminum. The effects of aluminum were evaluated on cytokine secretion and transporter expression. The role of aluminum kinetics parameters was studied in Caco-2 using transport inhibitors and in human colon biopsies by assessing genetic polymorphisms of transporters.
Results: Aluminum exposure was shown to induce cytokine secretion in colon of CD but not healthy patients. In Caco-2 cells, aluminum internalisation was correlated with inflammatory status. In human colon, analysis of genetic

Abbreviations: ABCD1, ATP binding cassette subfamily D member 1; AlCi, aluminum citrate; Alu-Rho, aluminum-rhodamine; *ATP*, adenosine triphosphate; BSA, Bovine Serum Albumin; CD, Crohn's Disease; cDNA, complementary deoxyribonucleic acid; CPZ, chlorpromazine; Ct, cycle threshold; CTCF, corrected total cellular fluorescence; Cyclo A, Cyclosporine A; *DMT1*, Divalent Metal Transporter 1; DRA, downregulated in adenoma; *GWAS*, genome-wide association study; qPCR, real-time polymerase chain reaction; IBD, inflammatory Bowel diseases; IL, Interleukine; MDR1, multidrug resistance protein 1; *MRP2*, multidrug resistance-associated protein 2; NGS, next-generation sequencing; NLRP3, NOD-like receptor family, pyrin domain containing 3; Polr2a, RNA polymerase II subunit A; RNA, ribonucleic acid; ROI, region of interest; SEM, standard error of the mean; SLC26A3, solute carrier family 26 member 3; SNP, single nucleotide polymorphism; TNF, Tumor necrosis factor; TER, transepithelial electrical resistance; UC, ulcerative colitis.

* Corresponding author at: Faculté de Médecine, Pôle recherche, Place Verdun, 59045 Lille Cedex, France.
E-mail address: cecile.vignal2@univ-lille.fr (C. Vignal).

http://dx.doi.org/10.1016/j.scitotenv.2022.158017
Received 29 March 2022; Received in revised form 9 August 2022; Accepted 9 August 2022
Available online 13 August 2022

polymorphisms and expression of *ABCB1* and *SLC26A3* transporters showed that their decreased activity was involved in aluminum-induced inflammation.

Conclusions: We hypothesize that alteration in detoxifying response would lead to a deregulation of intestinal homeostasis and to the expression of IBD. Our study emphasizes the complexity of gene/environment interaction for aluminum adverse health effect, highlighting at risk populations or subtypes of patients. A better understanding of correlations between gene expression or SNP and xenobiotic kinetics parameters would shift the medical paradigm to more personalized disease management and treatment.

1. Introduction

Inflammatory bowel disease (IBD) is a heterogeneous state of chronic intestinal inflammation comprising two main clinical phenotypes, Crohn's disease (CD) and ulcerative colitis (UC), distinguished by symptoms, location of inflammation and histological features (Torres et al., 2017; Ungaro et al., 2017). IBD is characterized by chronic relapsing inflammation of the gastrointestinal tract alternating acute episodes and remission. IBD are complex multifactorial diseases, originated from an interplay between the gut microbiota and, environmental and immunological factors, in genetically susceptible individuals, which promotes dysregulated innate and adaptive immune responses (de Souza and Fiocchi, 2016). Genome-wide association studies identified >250 IBD-associated genes, including genes related to epithelial barrier function, immune tolerance and mucosal defence or solute transport (Khor et al., 2011; Rivas et al., 2011). Although the exact etiopathology of IBD remains unknown, the key role of environmental factors in their pathogenesis is recognized. Indeed, the spatial heterogeneity of IBD, their increasing incidence and prevalence with time and in different regions around the world, the low concordance rate in monozygotic twins and the increased risk among migrants from low-incidence to high-incidence areas strengthens this idea (Molodecky et al., 2012; Ng et al., 2013; Vedamurthy and Ananthakrishnan, 2019). IBD first developed in western countries, however, recent data have described an increasing incidence in Eastern regions (Ng, 2014). This emergence of IBD in low-prevalence regions has accompanied the process of industrialization which is associated with modification of diet habit or increase of environmental pollutant exposure. We previously demonstrated that oral administration of aluminum worsened intestinal inflammation in mice models of IBD (Pineton de Chambrun et al., 2014). Aluminum was shown to have a deleterious impact on intestinal homeostasis. Indeed, mechanistically, aluminum induced inflammatory cytokines expression in the colon of mice and in the Caco-2 and HT-29 cancerous cell lines, decreased intestinal epithelial cells proliferation and impaired intestinal barrier function in mice (Djouina et al., 2016; Jeong et al., 2020b; Pineton de Chambrun et al., 2014). Aluminum exposure is thus suspected to be involved in IBD development. Aluminum is the most frequent metal in the earth's crust. Its presence is ubiquitous in nature, thus it can naturally contaminate food. It is also largely used in daily life products as food additive, in kitchenware or packaging (Vignal et al., 2016). In Europe, it was estimated that the tolerable weekly intake of 2 mg/kg bw of aluminum is exceeded in a significant proportion of the population, especially in children, who are more vulnerable to toxic effects of pollutants than adults (Arnich et al., 2012; Sirot et al., 2018). As aluminum oral bioavailability is <1 %, colonic epithelial cells are important target for aluminum adverse effect (Powell et al., 1994; Yokel and Florence, 2008). The gastrointestinal tract is chronically exposed to mixtures of xenobiotic substances including diet, pharmaceuticals or environmental contaminants. The human body has developed extensive molecular mechanisms to protect against the toxicity of those xenobiotics. Usually linked to liver metabolism, the intestine also expresses phase I and phase II enzymes as well as transporters to mediate biotransformation and excretion of xenobiotics (Bourgine et al., 2012). A strongly diminished expression of the ABC-transporter *ABCB1* (encoding the multidrug resistance protein 1 (MDR1), also known as permeability-glycoprotein 1 (P-gp)) was first shown in mucosal biopsies from UC patients (Langmann et al., 2004). Afterwards, profound alterations in transportome profiling have been highlighted in CD patients (Pérez-Torras et al., 2016). Defective mucosal detoxification system has been proposed to be part of the pathophysiology of IBD (Langmann and Schmitz, 2006). Indeed, variation of xenobiotic metabolizing enzymes or transporters, directly or indirectly involved in xenobiotic detoxification, could explain the differences in susceptibility to IBD development as well as the heterogeneity of response to xenobiotics observed in different populations.

In this manuscript, we studied aluminum adverse effects on human colon biopsies and assessed the involved mechanisms particularly in term of transport and subcellular localization. We hypothesize that an improper detoxification of aluminum implicating transporters might lead to an increased susceptibility to aluminum toxicity in IBD patients.

2. Materials and methods

2.1. Human colon biopsies stimulation

All subjects were recruited from the Department of Gastroenterology, Claude Huriez University Hospital, Lille, France and written informed consent was obtained. This study has been approved by the local institutional ethics committee (n° 2010-A00056–33). Participation in the study was proposed to all patients when the performance of a colonoscopy was needed for clinical assessment, required for the diagnosis or the follow-up of their intestinal disease. Control subjects were selected among patients who underwent colonoscopy as part of their clinical investigation for various reasons not related to inflammatory bowel disease. Two colonic biopsies were taken during colonoscopy from the same mucosal area from 51 Crohn's disease patients and 31 controls, as well as a blood sample.

Immediately after collection, biopsies were incubated in RPMI supplemented with 1 % Penicillin-Streptomycin and 0.1 % Fungizone (Thermo Fisher Scientific) and stimulated with 100 μg/ml aluminum citrate (AlCi) (Sigma-Aldrich) for 6 or 24 h. The dose used in our study, 100 μg/ml corresponding to 3.7 mM, is in the same order of concentration compared to other studies working on intestinal epithelial cell lines (Aspenström-Fagerlund et al., 2009; Jeong et al., 2020b, 2020a). Aluminum-treated biopsies were compared to unstimulated biopsies (termed NT for non-treated in the figures) incubated in the same medium without aluminum. After culture at 37 °C in a humidified atmosphere (95 % air and 5 % CO2), supernatants and cells were collected separately and stored at −80 °C until analysis.

2.2. Cytokine quantification

Three key cytokines involved in CD pathogenesis, TNFα, IL17A and IL1β, were quantified in the culture supernatant using a Human Magnetic Luminex Assay (Bio-Techne) according to the manufacturer's instructions. Samples were analyzed with the Bio-Plex 200 system and data were processed using Bio-Plex Manager software (Bio-Rad). Cytokine secretion was expressed according to the total quantity of proteins in cell supernatant determined using the DC™ protein assay kit (Bio-Rad). A calibration kit was run to standardize fluorescence signal before each experiment and a validation kit ensuring performance of fluidics and optics systems was run monthly. Patients for which cytokine secretion was below the limit of quantification were not included in statistical analysis.

2.3. In vitro intestinal barrier model

The human colon adenocarcinoma Caco-2 cell line (ATCC® HTB-37TM) was used to obtain an *in vitro* intestinal barrier model. Indeed, caco-2 cells have the ability to differentiate into a monolayer mimicking the intestinal epithelium when grown on transwell inserts. Caco-2 cells were maintained in complete medium (DMEM with phenol red and 4.5 g/l D-(+)-glucose, supplemented with 1 % (v/v) penicillin/streptomycin, 1 % (v/v) Glutamax, Thermo Fisher Scientific, and 10 % (v/v) heat inactivated fetal bovine serum, Eurobio Scientific) at 37 °C in a humidified atmosphere of 5 % CO2/95 % air. To differentiate Caco-2 cells into a polarized monolayer with an apical brush border, cells were cultivated on polyester (PET) microporous filter with 3 μm of pore size in 24 or 6-well transwell plates (Falcon® Permeable Support 353492). Briefly, 85000 cells/cm^2 were seeded with complete medium on the apical side and complete medium without cells were added in the basal side of the Transwell insert. After 21 days of culture, Caco-2 cells were differentiated and polarized, resembling the morphological and functional features of the mature enterocytes. To verify epithelial integrity of cell monolayers, Transepithelial Electrical Resistance (TER) was measured with an Epithelial Voltohmmeter (EVOM2) coupled to a chopstick electrode pair (STX2, both World Precision Instruments, Sarasota, FL, USA).

2.4. Caco-2 exposure to aluminum

Two different experiments were performed to document the impact of aluminum citrate on epithelial barrier. We first assessed the impact of aluminum on the ability of Caco-2 cells to differentiate and form an impermeable monolayer. One day after seeding Caco-2 cells on Transwell inserts, medium in apical side was replaced by complete medium supplemented with 100 μg/ml of aluminum citrate (AlCi) for 15 days. Untreated cells received complete medium without aluminum citrate. Epithelial integrity of cell monolayers was monitored from day 0 to day 15 by TER measuring. At the end of the exposure period, cells were collected for further analysis.

In a second set of experiments, we evaluated the ability of aluminum to disturb a differentiated monolayer. Caco-2 cells were seeded on Transwell inserts and left to differentiate for 21 days. At day 21, cells were washed with PBS 1× and complete medium containing 100 μg/ml aluminum citrate or aluminum-rhodamine was added in apical compartment. Untreated cells received complete medium only. After 6 or 24 h of exposure, supernatants (basal and apical side) were collected for fluorescence intensity measurement ($n = 8$), cells were washed with PBS 1× for RNA extraction ($n = 5$) or directly fixed with 10 % buffered formalin for confocal microscopy ($n = 3$).

2.5. Size measurement of aluminum citrate and aluminum-rhodamine

The size of aluminum citrate and aluminum-rhodamine was measured by dynamic light scattering in pure water at 25 °C. Measurements were carried out in triplicate using a zetasizer nanoZS (Malvern Instruments, France) with a particle concentration of 100 μg/ml.

2.6. Caco-2 cells monolayers exposure to aluminum-rhodamine and treatment with transport inhibitors

After 21 days of differentiation, Caco-2 cells monolayers were treated in apical side for 1 h with chlorpromazine (CPZ) at 10 μg/ml ($n = 7$), Filipin III at 10 μg/ml (n = 7) or Cyclosporine A (Cyclo A) at 1 μg/ml (n = 7) diluted in complete medium (Sigma-aldrich). After 1 h of treatment with transport inhibitor, all group were exposed in apical side with 100 μg/ml of aluminum-rhodamine (Alu-Rho) for 6 h. Untreated cells received complete medium only ($n = 7$). At the end of the exposure period, supernatants (basal and apical side) were collected for fluorescence intensity measurement, cells were washed with PBS 1× for RNA extraction ($n = 4$) or directly fixed with 10 % buffered formalin (Microm Microtech) for confocal microscopy ($n = 3$).

2.7. Fluorescence intensity measurement in supernatant

To measure fluorescence intensity of aluminum-rhodamine in each compartment of transwell, 100 μl of supernatant were transferred in a 96 well black plate and read in a microplate reader (FLUOstar Omega BMG labtech) at 510 nm excitation wavelength and 568 nm fluorescence emission.

2.8. Confocal microscopy and aluminum-rhodamine sub-cellular quantification

Caco-2 cells incubated with aluminum-rhodamine were fixed in 10 % buffered formalin for 30 min, processed, and embedded in paraffin wax by automatic sample preparation system (LOGOS One, Milestone). Serial histological sections of 5 μm thickness were cut, deparaffinized and rehydrated.

For immunohistochemistry of actin, sections were placed in 10 mM sodium citrate buffer pH 6.0 and incubated in a heat-induced antigen retrieval chamber for 20 min at 121 °C. After washing, sections were blocked for 30 min with 5 % BSA in PBS, stained overnight at 4 °C with anti-β-Actin antibody (1/500, A5441 Sigma-Aldrich) and incubated with Alexa-488 conjugated secondary antibody (1/500, A28175, Thermo Fischer Scientific) for 1 h. Sections were counterstained with Hoechst 33342 (1/1000, molecular Probes).

Ten images were acquired using an LSM 710 confocal laser-scanning microscope (Carl Zeiss) equipped with 63×/1.4 immersion oil objective. Hoechst 33342, Alexa-488 and aluminum-Rhodamine were imaged using UV, Argon 488 and 561 nm diode-pumped solid-state laser. Images were processed with ZEN software.

To quantify aluminum-rhodamine, we followed the method described by Mc Cloy R.A et al. (McCloy et al., 2014). Using FIJI software, a ROI was drawn around each cell compartment (apical side with microvilli brush borders, cytoplasm, nucleus and basal side with filter) and area, integrated density, mean fluorescence were measured, along with several adjacent background readings. The corrected total cellular fluorescence (CTCF) was calculated as followed: CTCF = integrated density – (area of selected cell compartment × mean fluorescence of background readings) (Schindelin et al., 2012).

2.9. Real-time quantitative PCR

Total RNA was extracted from Caco-2 and colon biopsies with the NucleoSpin RNA commercial kit as described by the manufacturer (Macherey-Nagel). cDNA was synthesized with the High Capacity cDNA Reverse Transcription kit and qPCR was performed with SyBrGreen fluorescence detection in a StepOne system (Thermo Fisher Scientific). The primer sequences were designed using Primer3Web and are available upon request. Melting curve analyses were performed for each sample and gene to confirm the specificity of the amplification. The relative expression of each target gene was normalized to the relative expression of the Polr2a gene. The quantification of the target gene expression was based on the comparative cycle threshold (Ct) value. The fold changes of the target genes were analyzed by the $2-\Delta\Delta Ct$ method.

2.10. Sequencing analysis

Genomic DNA was extracted from blood samples using the NucleoSpin Blood Kit from Macherey-Nagel according to manufacturer protocol. AmpliSeq libraries were prepared using an ion AmpliSeq library kit 2.0 and ion AmpliSeq custom panel (Life Technologies). AmpliSeq technologies were used to design a custom NGS library. Ten ng of each DNA sample was used as a template to prepare the library. Quality control of all libraries was performed with an Agilent bioanalyser using high sensitivity chips. Library templates were amplified clonally using an IonChef, following the manufacturer's protocol. Samples were subjected to the Ion S5 sequencer using Ion 540 chips and Ion 540 kit-Chef (Life Technologies). Fifty-four barcoded samples were loaded per chip to ensure an average depth of 1500, on 2

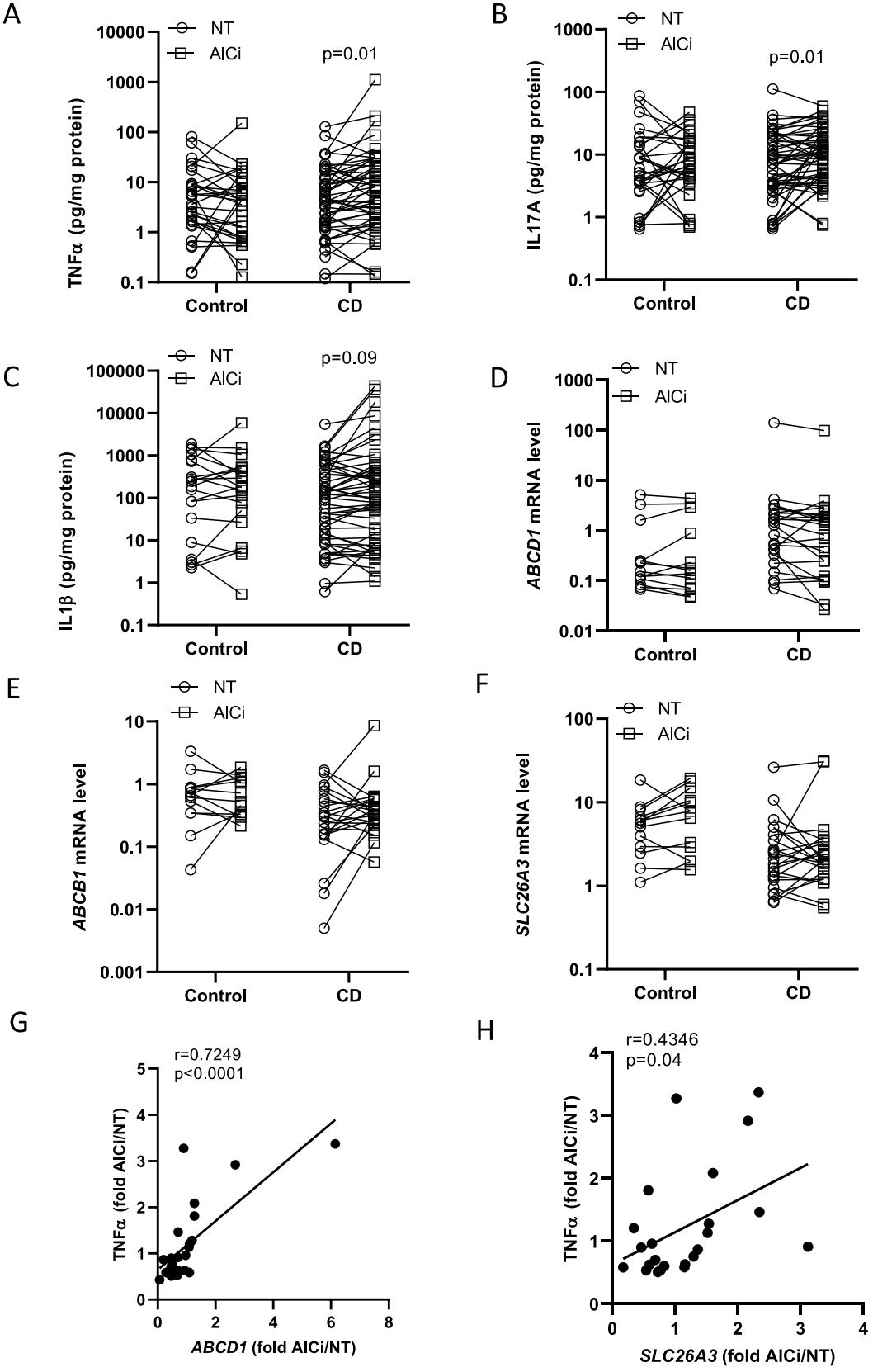

Fig. 1. Effect of aluminum on cytokine secretion and transporter expression in human colon biopsies. Human colon biopsies isolated from Crohn's Disease (CD) and control patients were incubated with (AlCi) or without (NT) aluminum citrate and secretion of TNFα (A), IL17A (B) and IL1β (C) was assessed in culture supernatants (control, $n = 31$ *vs* CD $n = 51$). mRNA expression of ABCD1 (D), ABCB1 (E) and SLC26A3 (F) was assessed in biopsies (control, $n = 15$ *vs* CD $n = 24$). Results from unstimulated and stimulated biopsy from the same patient are paired in the graphs. Statistical analysis was performed between unstimulated and stimulated biopsy from the same patient and traduce the ability of aluminum to modify cytokine secretion or transporter expression. Fold expression of ABCD1 (G) or SLC26A3 (H) and TNFa induced by aluminum in CD patients' biopsies were plotted and Pearson correlation was calculated.

Ion chips. For data analysis, alignment of the sequences to the human genome build 19 reference genome and base calling were performed using Torrent Suite software. Identification of variants was performed with an ion torrent variant caller and coverage analysis was generated using coverage analysis plugins (Life Technologies).

2.11. Statistical analysis

Data are presented as the mean ± SEM. Comparison between different treatment groups was performed using the Mann–Whitney test. Analyses were performed using the GraphPad Prism5 Software. Statistical significance was defined as $p < 0.05$. For all experiments, $*p < 0.05$, $**p < 0.01$, $***p < 0.005$, $****p < 0.001$.

3. Results

3.1. Analysis of aluminum induced inflammation and expression of transporters in human colon biopsies

Human intestinal biopsies isolated from Crohn's Disease (CD) patients ($n = 51$) and controls ($n = 31$) were stimulated with AlCi for 24 h and cytokine secretion was assessed in culture supernatants. Paired statistical analysis between untreated (NT) and AlCi treated gut biopsies revealed that AlCi induced significant TNFα and IL17a secretion and a trend toward a significant secretion of IL1β in CD patients but not in control biopsies (Fig. 1A-C).

The mRNA expression of several transporters was also analyzed in biopsies, and no modification of their expression following AlCi treatment was observed whether in CD patients or in controls (Fig. 1D-F). However, we noticed a positive correlation between the expression of *TNFa* and the one of *ABCD1 (ATP binding cassette subfamily D member 1)* and *SLC26A3 (solute carrier family 26 member 3*, encoding the down-regulated in adenoma protein, DRA) in CD patients (Fig. 1G and H). To test whether aluminum transport and localisation are important for its proinflammatory effect, we assessed this mechanism in the model of Caco-2 cells.

3.2. Study of aluminum effect on gut epithelial barrier

Caco-2 cells are human intestinal carcinoma cell line which have the ability to differentiate into a monolayer mimicking the intestinal epithelium when grown on transwell inserts. This monolayer shows a strong physical barrier as denoted by the increase of the transepithelial resistance (TER) over time during their differentiation (Fig. 2A, black line). We first wanted to describe aluminum effects on the intestinal barrier. Incubation of undifferentiated Caco-2 cells with 100 μg/ml AlCi impaired barrier formation, as evidenced by a significant difference in TER from day 8 compared to unstimulated cells and an inability to stabilize an impermeable monolayer (Fig. 2A). Once polarized (i.e. after 10 day differentiation), incubation of Caco-2 cell monolayers with AlCi increased intestinal permeability, as evidenced by a significant mitigation of TER, and *OCCLUDIN* and *CLAUDIN-7* mRNA levels compared to unstimulated cells (Fig. 2B and C).

We then tested the same parameters with a laboratory-made engineered fluorescent form of aluminum, composed of a rhodamine containing core and an $Al(OH)_3$ shell (Alu-Rho) (Khan et al., 2013). We first analyzed the size distribution of Alu-Rho and AlCi. Alu-Rho and AlCi solutions showed a homogeneous size distribution with a mean particle size of 615 nm for Alu-Rho and 532 nm for AlCi (Fig. 2D). Incubation of differentiated Caco-2 cells with 100 μg/ml Alu-Rho led to a significant decrease in TER and *OCCLUDIN* and *CLAUDIN-7* expression (Fig. 2E and F), indicating that Alu-Rho reproduces the ability of AlCi to perturbate gut epithelial barrier.

3.3. Analysis of aluminum cellular localisation and transport

In order to further assess aluminum behavior in term of transport or cellular localization, we took advantage of the fluorescence of aluminum-rhodamine. We first followed the appearance of fluorescence in the basal

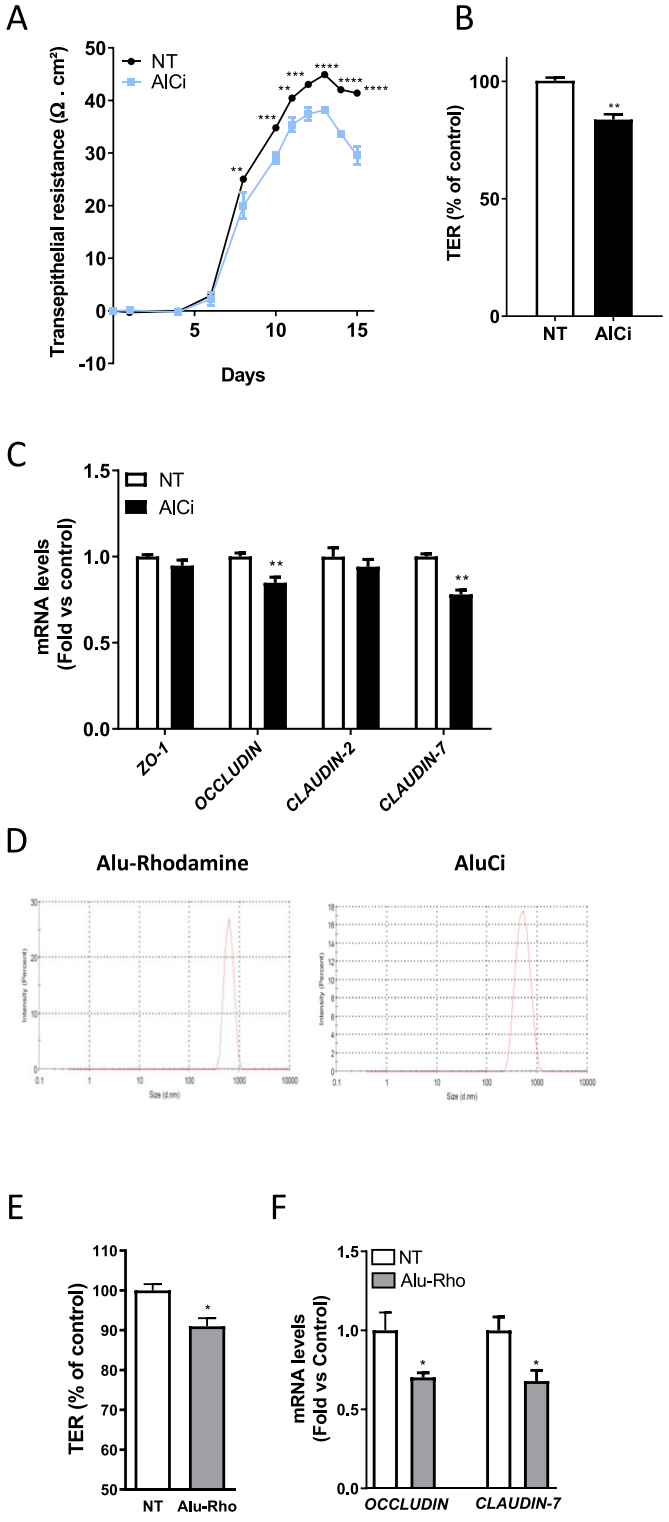

Fig. 2. Effect of aluminum on gut epithelial barrier parameters in Caco-2 cells. (A) Undifferentiated Caco-2 cells were incubated with (AlCi) or without (NT) aluminum citrate for 15 days and transepithelial resistance was assessed over time. Differentiated Caco-2 cells were incubated with (AlCi) or without (NT) aluminum citrate for 6 h and transepithelial resistance (TER) (B), and mRNA expression of cellular junctions (C) were assessed. (D) Size distribution of aluminum-rhodamine and AlCi was assessed with a nanosizer. Differentiated Caco-2 cells were incubated with (Alu-Rho) or without (NT) Alu-Rho for 3 h and transepithelial resistance (TER) (E), and mRNA expression of cellular junctions (F) were assessed. Statistical analysis was performed by comparing aluminum treated cells to the non-treated condition.

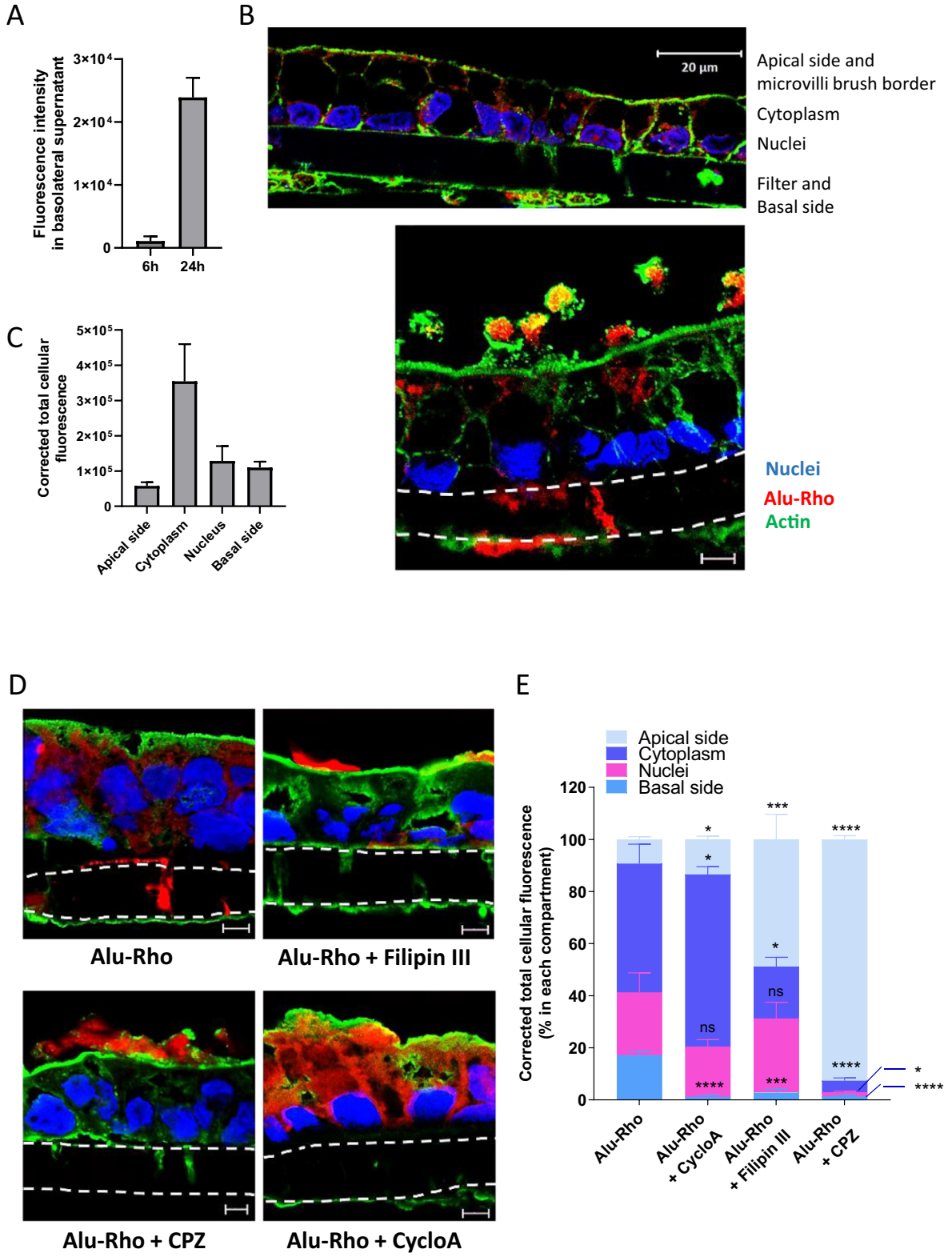

Fig. 3. Analysis of aluminum cellular localisation in Caco-2 cells. Differentiated Caco-2 cells were incubated with Alu-Rho for 6 and 24 h and fluorescence was measured in basolateral supernatant (A) and quantified in the apical side, in the cytoplasm, in the nucleus and in the basal side on histological slides (B and C). Actin was revealed by immunohistochemistry and nuclei by Hoechst 33342 staining. Differentiated Caco-2 cells were incubated with transport inhibitors (Filipin III, chlorpromazine (CPZ) or Cyclosporine A (Cyclo A)) for 1 h and then treated with Alu-Rho for 6 h. (D) Confocal microscopy was performed to visualize aluminum cellular localisation. (E) Fluorescence was measured in each compartment. Images were acquired using an LSM 710 confocal laser-scanning microscope (Carl Zeiss) equipped with 63 × /1.4 immersion oil objective. Images were processed with ZEN software. If not mentioned, scale bar = 5 µm. Statistical analysis was performed by comparing fluorescence in one compartment of cells treated with Alu-Rho and inhibitors to the fluorescence in the same compartment of cells treated with Alu-Rho alone.

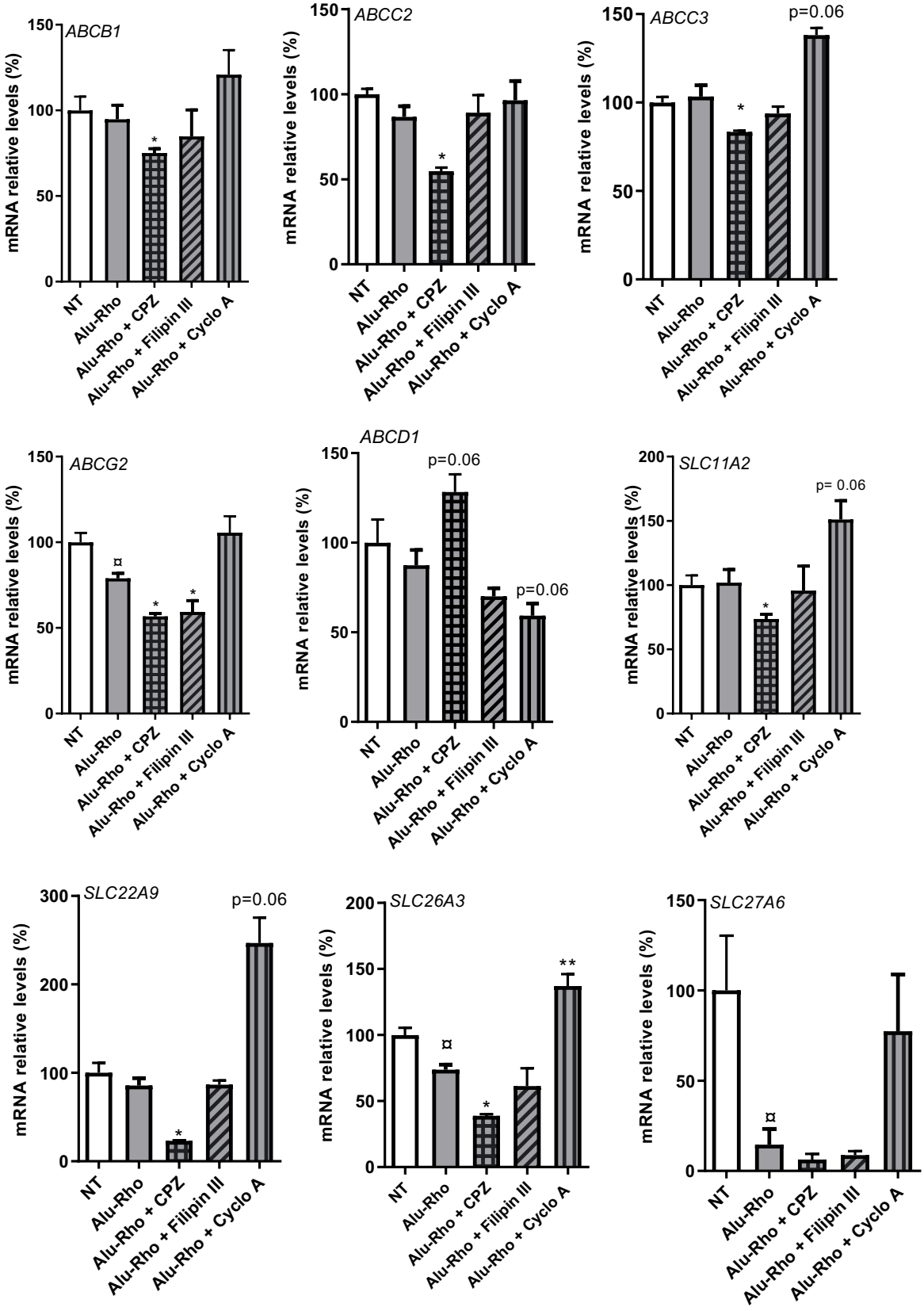

Fig. 4. Effect of Filipin III, chlorpromazine or Cyclosporine A and aluminum incubation on transporter expression in Caco-2 cells. Differentiated Caco-2 cells were incubated with transport inhibitors (Filipin III, chlorpromazine (CPZ) or Cyclosporine A (Cyclo A)) for 1 h and then treated with Alu-Rho for 6 h. mRNA expression of ABCB1, ABCC2, ABCC3, ABCG2, ABCD1, SLC11A2, SLC22A9, SLC26A3 and SLC27A6 was then assessed. The open stars (¤) show statistically significant differences between the non-treated (NT) condition (white bar) and the Alu-Rho treated cells (grey bars). The stars (*) show statistically significant differences between Alu-Rho treated cells (grey bars) and Alu-Rho + inhibitors groups (patterned bars). Actual *p*-values show a trend toward a significant difference between Alu-Rho treated cells (grey bars) and Alu-Rho + inhibitors groups (patterned bars).

compartment of transwell inserts after 6 and 24 h stimulation with Alu-Rho and observed a time-dependent increase of fluorescence, showing the crossing of the Caco-2 cell layer by Alu-Rho (Fig. 3A). This was further confirmed by confocal microscopy observation and image fluorescence quantification which showed Alu-Rho in the apical and basal sides of the cells, between cells and in the cytoplasm and nuclei of cells (Fig. 3B and C). In some images, we were also able to see some Alu-Rho particles surrounded by actin extensions. We then addressed the mechanisms by which aluminum could enter and cross the cells. We thus tested the endocytic pathway using two different inhibitors, chlorpromazine (CPZ), which inhibits clathrin-mediated endocytosis, and Filipin III, which inhibits lipid rafts-mediated endocytosis (Ding et al., 2021). We also evaluated the influence of the broad-spectrum transport modulator cyclosporine A (Cyclo A) on Alu-Rho subcellular localization (Qadir et al., 2005). Confocal microscopy observation and image fluorescence quantification showed that the amount of Alu-Rho was significantly higher in the apical compartment and conversely less important in the cytoplasm, nuclei and basal compartments when cells were incubated with CPZ or Filipin III, reflecting that Alu-Rho is retained at the apical side of cells (Fig. 3D and E). Conversely, we evidenced that incubation of cells with Cyclo A induced Alu-Rho retention in the cytoplasm. Indeed, almost 93 % of Alu-Rho was found inside the cells under Cyclo A incubation (Fig. 3E).

We then assessed the influence of CPZ, Filipin III and Cyclo A on several transporter expression; *ABCB1*, *ABCC2* (encoding the multidrug resistance-associated protein 2, MRP2), *ABCC3* (encoding the MRP3 protein), *ABCD1*, *ABCG2, SLC11A2* (encoding the natural resistance-associated macrophage protein 2, NRAMP2, also known as divalent cation transporter 1, DMT1), *SLC22A9, SLC26A3* and *SLC27A6* (encoding the long-chain fatty acid transport protein 6). We first showed that Alu-Rho decreased the expression of *ABCG2, SLC26A3* and *SLC27A6* but had no effect on the expression of other receptors (*ABCB1, ABCC2, ABCC3, ABCD1, SLC11A2* or *SLC22A9*) compared to untreated cells (Fig. 4 grey bars). We also found that CPZ had a profound effect on the expression of almost all the transporters tested by decreasing their expression compared to cells stimulated with Alu-Rho alone (Fig. 4 squared grey bars). The effect of Filippin III or Cyclo A incubation was more mitigated with a significant decrease in *ABCG2* and increase in *SLC26A3* expression compared to cells stimulated with Alu-Rho alone respectively (Fig. 4 hatched and lined grey bars). A trend toward a modification of *ABCC3, ABCD1, SLC11A2* and *SLC22A9* expression was also observed after Cyclo A incubation (Fig. 4 lined grey bars).

3.4. Study of the consequences of aluminum subcellular localisation on inflammation

As a positive correlation was observed between transporter and inflammation in human gut biospsies, we assessed whether aluminum localization would have an impact on Caco-2 inflammatory status. We previously published that aluminum stimulation of Caco-2 cells induced *IL1β* expression (Pineton de Chambrun et al., 2014). We confirmed this observation; incubation of Caco-2 cells with Alu-Rho induced the expression of *IL1β*, the mediator of IL1β activation *NLRP3* and *TNFα* compared to untreated cells (Fig. 5 grey bars). In the presence of CPZ or Filipin III, Alu-Rho failed to induce inflammation, as *TNFα*, *IL1β* and *NLRP3* expressions were decreased compared to Alu-Rho stimulated cells reaching the expression of untreated cells (Fig. 5 squared and hatched grey bars). Conversely, Cyclo A incubation of cells further increased inflammation as TNFα, IL1β and NLRP3 expression was higher than with Alu-Rho alone (Fig. 5 lined grey bars).

3.5. Correlation between inflammation and genetic polymorphisms of transporter genes in human colon biopsies

More than 240 risk gene loci have been associated with IBD (McGovern et al., 2015). Among them single nucleotide polymorphisms have been identified in xenobiotic transporters such as *ABCB1* which is the most studied one (Potočnik et al., 2004; Weersma et al., 2007). We thus decided to analyse the impact of aluminum treatment on human gut biopsies according to *ABCB1* polymorphism status. We found that 53 % of our CD population carries a heterozygous (A/G) genotype and 20 % a homozygous variant allele (G/G). We also found that the increase of TNFα secretion following aluminum stimulation was only observed in patients carrying hetero- or homozygous mutated allele in *ABCB1* gene (Fig. 6A). *SLC26A3* polymorphisms were also associated with IBD (Shao et al., 2018). We thus analyzed TNFα secretion according to *SLC26A3* genotype. We observed that 46 % of our CD cohort carried a heterozygous genotype (G/A) and 16 % a

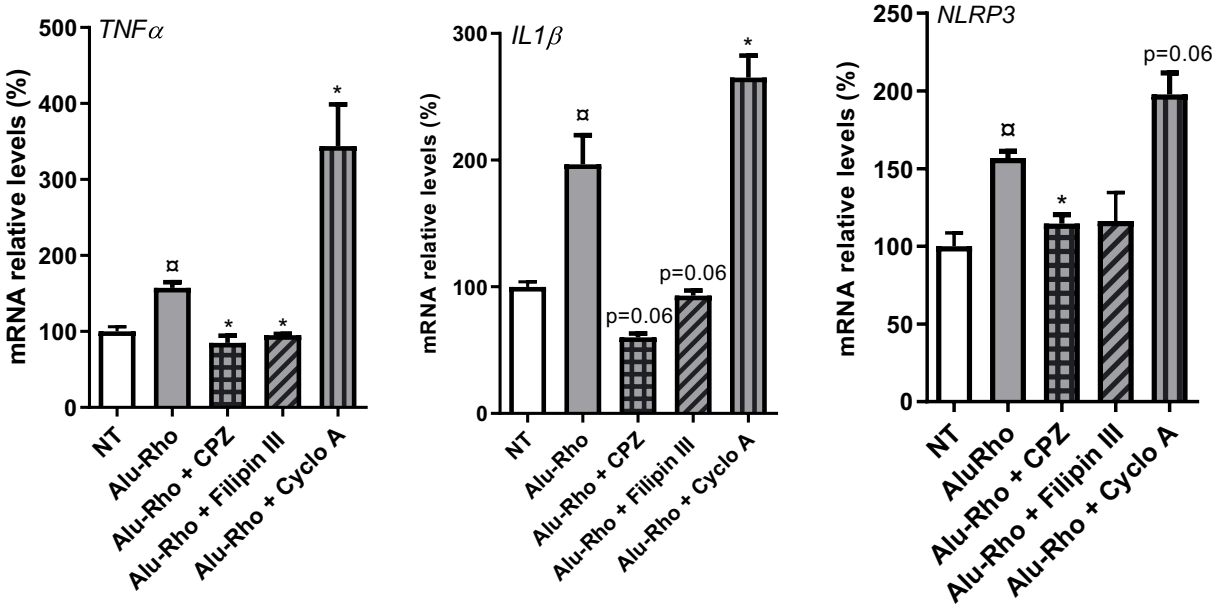

Fig. 5. Effect of Filipin III, chlorpromazine or Cyclosporine A and aluminum incubation on inflammatory marker expression in Caco-2 cells. Differentiated Caco-2 cells were incubated with transport inhibitors (Filipin III, chlorpromazine (CPZ) or Cyclosporine A (Cyclo A)) for 1 h and then treated with Alu-Rho for 6 h. mRNA expression of TNFα, IL1β and NLRP3 was assessed. The open stars (¤) show statistically significant differences between the non-treated (NT) condition (white bar) and the Alu-Rho treated cells (grey bars). The stars (*) show statistically significant differences between Alu-Rho treated cells (grey bars) and Alu-Rho + inhibitors groups (patterned bars). Actual p-values show a trend toward a significant difference between Alu-Rho treated cells (grey bars) and Alu-Rho + inhibitors groups (patterned bars).

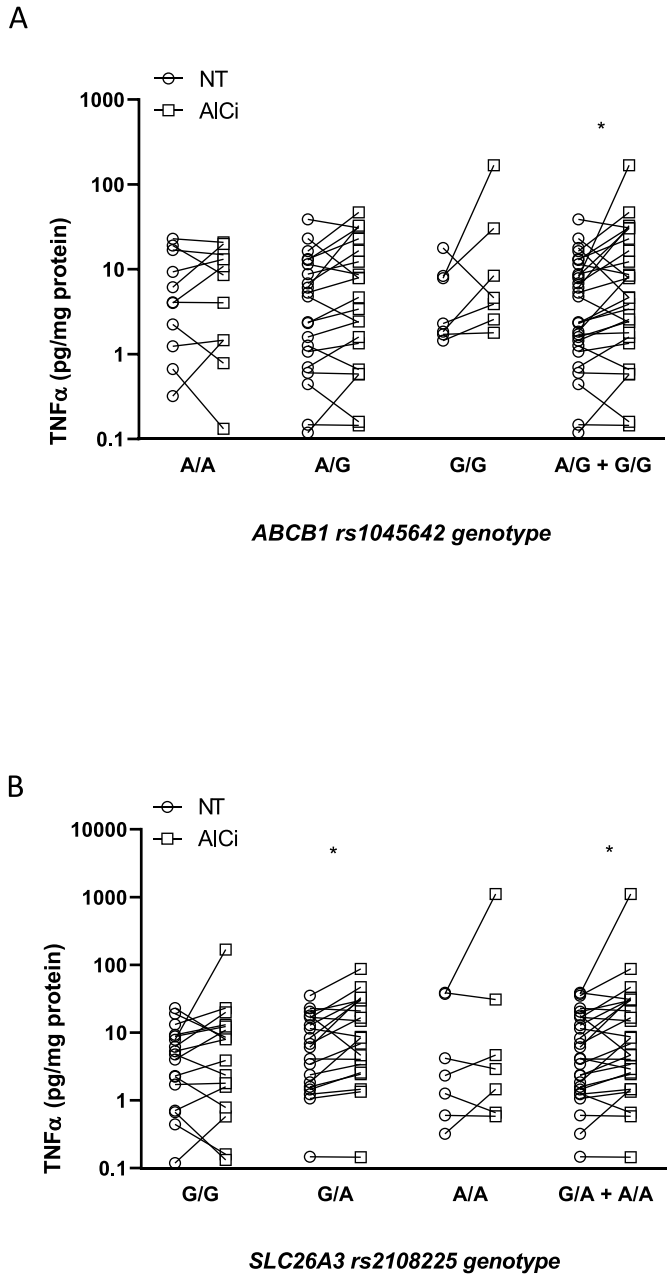

Fig. 6. Effect of Aluminum on TNFα secretion in CD colon biopsies according to MDR1 or SLC26A3 genotype. Human colon biopsies isolated from Crohn's Disease (CD) patients were incubated with (Alu) or without (NT) aluminum citrate for 24 h and secretion of TNFα was assessed in culture supernatants and plotted according to ABCB1 (A) or SLC26A3 (B) genotype. For ABCB1, A/A represents the reference genotype and G/G the allelic variant. For SLC26A3, G/G represents the reference genotype and A/A the variant. Results from unstimulated and stimulated biopsy from the same patient are paired in the graphs. Statistical analysis was performed between unstimulated and stimulated biopsy from the same patient and traduce the ability of aluminum to modify TNFα secretion.

homozygous variant allele (A/A). A similar observation was done as for *ABCB1* polymorphism. Indeed, aluminum induced TNFα secretion only in CD patients carrying hetero- or homozygous variant (Fig. 6B).

4. Discussion

We previously demonstrated that aluminum administration impaired intestinal barrier function and aggravated colitis symptoms in mice models of IBD, suggesting that aluminum might be an environmental risk factor for IBD (Djouina et al., 2016; Pineton de Chambrun et al., 2014). In this study, we wanted to reinforce these results by studying the inflammatory impact of aluminum exposure in human gut biopsies and a potential mechanism involving the xenobiotic detoxification system.

We showed that aluminum induced inflammatory cytokine secretion in gut biopsies isolated from CD patients but not in healthy biopsies, suggesting that CD patients are more susceptible to the deleterious effects of aluminum. Transporter expression was not modified following aluminum treatment but was correlated with inflammatory status suggesting a link between aluminum transport and inflammation. Such a link has been highlighted in animal models showing an impaired intestinal homeostasis in *Slc26a3* knock-out mice and a spontaneous development of colitis in *abcb1* deficient mice (Kumar et al., 2021; Panwala et al., 1998; Staley et al., 2009; Tanner et al., 2013). Further mechanistic analysis in Caco-2 cells showed a modified aluminum distribution following incubation with the clathrin-mediated endocytosis inhibitor chlorpromazine, the lipid rafts-mediated endocytosis inhibitor Filipin III or the broad spectrum transporter inhibitor cyclosporine A. This suggested that aluminum internalisation can occur through different pathways. The divalent Metal Transporter 1 (DMT1), coded by the *SLC11A2* gene, has been shown to specifically transport aluminum in plants (Li et al., 2014). Its role in aluminum induced toxicity has been suggested in neurodegenerative disorders in the *Caenorhabditis elegans* model (VanDuyn et al., 2013). To date, no data exist about its role in aluminum transport in mammals or in intestinal homeostasis. In our study, *SLC11A2* expression was not modified by aluminum treatment neither in human biopsies nor in Caco-2 cells. The role of DMT1 in aluminum transport and toxic effect in mammals would deserve more specific studies.

Confocal microscopy showed that following apical exposure, aluminum was localized in the cytoplasm and nucleus. This was accompanied by an increased expression of NLRP3 and IL1β. NLRP3 is an intracellular pattern recognition receptor activated by pathogen-associated molecular patterns as well as bacterial RNA, ATP, silica crystals or aluminum (Eisenbarth et al., 2008; Hornung et al., 2008; Kanneganti et al., 2006; Li et al., 2008). Activation of NLRP3 triggers an inflammatory response leading to IL1β and IL18 secretion. However, the role of NLRP3 in the cellular effects induced by aluminum is controversial (Franchi and Núñez, 2008; Kuroda et al., 2011). Incubating cells with Cyclosporine A, which accumulated aluminum inside cells, further enhanced *NLRP3* and *IL1β* expression. Conversely, incubation of cells with chlorpromazine or Filipin III, which prevent aluminum from entering the cells, led to a down regulation of *NLRP3* and *IL1β* expression compared to aluminum treated cells. This suggest that the inflammatory effect of aluminum is mediated by the direct activation of NLRP3 by aluminum inside cells.

GWAS have identified >240 risk gene loci to be associated with IBD development, but their clinical utility remains limited and mechanisms that link genetic variants to disease expression are largely unknown. In our study, we identified that polymorphisms in *ABCB1* and *SLC26A3* genes influenced inflammatory response to aluminum in human gut biopsies. *ABCB1* encodes a member of the transporter family of proteins, P-glycoprotein. It functions as a transmembrane efflux pump to restrict xenobiotic accumulation in tissues and thereby protecting them from the chemical-induced toxicity (Wang et al., 2018). The rs1045642 polymorphism is the most studied genetic variant of *ABCB1*. The T allele of *MDR1* is associated with a lower P-glycoprotein expression in the gut, a decreased activity of the protein and an increased tissue concentration of drugs (Brinkmann and Eichelbaum, 2001; Hoffmeyer et al., 2000). *SLC26A3* encodes the ion transporter downregulated in adenoma (DRA) protein. DRA is involved in chloride absorption and in maintenance of epithelial homeostasis in the gut (Kumar et al., 2021). mRNA and protein expression of SLC26A3 were shown to be increased in the colon of patients carrying the AA genotype (Shao et al., 2018). Inter-individual variability of xenobiotics toxicity would not result only from sequence variants in genes. Polymorphisms in the xenobiotic transporter *ABCG2* were not associated with IBD onset, however, lower level of ABCG2 has been noticed in the mucosa of IBD patients (Englund et al., 2007; Erdmann et al., 2019). ABCG2 is localized at the apical membrane of intestinal epithelial cells, this transporter

is important for dealing with xenobiotics by mediating efflux of toxicants. Moreover, intestinal inflammation has been shown to interfere with ABCG2 expression (Deuring et al., 2011). In our study, we showed that aluminum treatment downregulated *ABCG2* expression and increased inflammation in Caco-2 cells. *ABCB1* and *SLC26A3* mutations or defect in *ABCG2* expression might increase aluminum load in cells, activate intracellular signaling, among which NLRP3, leading to inflammation.

Taken as a whole, we can hypothesize that the decreased activity of some transporters, either by genetic alteration or not, could prevent an appropriate detoxifying response, ultimately leading to a deregulation of intestinal homeostasis and to the expression of the pathology. Our study emphasizes the complexity of gene/environment interaction for xenobiotics adverse health effect, highlighting at risk populations or subtypes of patients. A better understanding of correlations between gene expression or SNP and xenobiotics kinetics parameters would shift the medical paradigm to more personalized disease management and treatment.

5. Conclusion

The present study showed that aluminum induced cytokine secretion in colon of CD but not healthy patients. We observed that internalisation of aluminum is correlated to inflammation. Genetic polymorphism of *ABCB1* or *SLC26A3* transporters increased susceptibility of colon to aluminum-induced inflammation, suggesting that alteration in detoxifying response might lead to IBD development.

CRediT authorship contribution statement

Madjid Djouina: Methodology, Formal analysis, Investigation, Writing - Original Draft. **Christophe Waxin:** Formal analysis, Investigation. **Frédéric Leprêtre:** Formal analysis, Writing - Original Draft. **Meryem Tardivel:** Methodology, Resources. **Olivier Tillement:** Resources. **Francis Vasseur:** Resources. **Martin Figeac:** Formal analysis, Resources. **Antonino Bongiovanni:** Resources. **Shéhérazade Sebda:** Investigation. **Pierre Desreumaux:** Funding acquisition. **David Launay:** Funding acquisition. **Laurent Dubuquoy:** Funding acquisition. **Mathilde Body-Malapel:** Conceptualization, Writing - Review & Editing, Supervision, Funding acquisition. **Cécile Vignal:** Conceptualization, Methodology, Validation, Formal analysis, Writing - Original Draft, Supervision, Funding acquisition, Project administration.

Grant support

This work was supported by the Hauts de France Region and the Ministère de l'Enseignement Supérieur et de la Recherche (CPER Climibio), the European Fund for Regional Economic Development and the Lille University Hospital.

Data availability

Data will be made available on request.

Declaration of competing interest

The authors declare the following financial interests/personal relationships which may be considered as potential competing interests:

Olivier Tillement reports a relationship with MexBrain that includes: board membership, employment, equity or stocks, and funding grants.

Acknowledgments

The authors thank the Hauts de France Region and the Ministère de l'Enseignement Supérieur et de la Recherche (CPER Climibio), the European Fund for Regional Economic Development and the Lille University Hospital for their financial support. The authors thank Rodolphe Carpentier for providing transport inhibitors. The authors also acknowledge the gastroenterologists and endoscopists from the Department of Gastroenterology, Claude Huriez University Hospital in Lille who contributed to include patients in the study. The authors thank the patients who accepted to participate to this study.

References

Arnich, N., Sirot, V., Rivière, G., Jean, J., Noël, L., Guérin, T., et al., 2012. Dietary exposure to trace elements and health risk assessment in the 2nd French total diet study. Food. Chem. Toxicol. 50, 2432–2449. https://doi.org/10.1016/j.fct.2012.04.016.

Aspenström-Fagerlund, B., Sundström, B., Tallkvist, J., Ilbäck, N.-G., Glynn, A.W., 2009. Fatty acids increase paracellular absorption of aluminium across Caco-2 cell monolayers. Chem. Biol. Interact. 181, 272–278. https://doi.org/10.1016/j.cbi.2009.06.016.

Bourgine, J., Billaut-Laden, I., Happillon, M., Lo-Guidice, J.-M., Maunoury, V., Imbenotte, M., et al., 2012. Gene expression profiling of systems involved in the metabolism and the disposition of xenobiotics: comparison between human intestinal biopsy samples and colon cell lines. Drug Metab. Dispos. 40, 694–705. https://doi.org/10.1124/dmd.111.042465.

Brinkmann, U., Eichelbaum, M., 2001. Polymorphisms in the ABC drug transporter gene MDR1. Pharmacogenomics J 1, 59–64. https://doi.org/10.1038/sj.tpj.6500001.

de Souza, H.S.P., Fiocchi, C., 2016. Immunopathogenesis of IBD: current state of the art. Nat. Rev. Gastroenterol. Hepatol. 13, 13–27. https://doi.org/10.1038/nrgastro.2015.186.

Deuring, J.J., de Haar, C., Koelewijn, C.L., Kuipers, E.J., Peppelenbosch, M.P., van der Woude, C.J., 2011. Absence of ABCG2-mediated mucosal detoxification in patients with active inflammatory bowel disease is due to impeded protein folding. Biochem. J. 441, 87–93. https://doi.org/10.1042/BJ20111281.

Ding, Y., Zhang, R., Li, B., Du, Y., Li, J., Tong, X., et al., 2021. Tissue distribution of polystyrene nanoplastics in mice and their entry, transport, and cytotoxicity to GES-1 cells. Environ. Pollut. 280, 116974. https://doi.org/10.1016/j.envpol.2021.116974.

Djouina, M., Esquerre, N., Desreumaux, P., Vignal, C., Body-Malapel, M., 2016. Toxicological consequences of experimental exposure to aluminum in human intestinal epithelial cells. Food Chem. Toxicol. 91, 108–116. https://doi.org/10.1016/j.fct.2016.03.008.

Eisenbarth, S.C., Colegio, O.R., O'Connor, W., Sutterwala, F.S., Flavell, R.A., 2008. Crucial role for the Nalp3 inflammasome in the immunostimulatory properties of aluminium adjuvants. Nature 453, 1122–1126. https://doi.org/10.1038/nature06939.

Englund, G., Jacobson, A., Rorsman, F., Artursson, P., Kindmark, A., Rönnblom, A., 2007. Efflux transporters in ulcerative colitis decreased expression of BCRP (ABCG2) and pgp (ABCB1). Inflamm. Bowel Dis. 13, 291–297. https://doi.org/10.1002/ibd.20030.

Erdmann, P., Bruckmueller, H., Martin, P., Busch, D., Haenisch, S., Müller, J., et al., 2019. Dysregulation of mucosal membrane transporters and drug-metabolizing enzymes in ulcerative colitis. J. Pharm. Sci. 108, 1035–1046. https://doi.org/10.1016/j.xphs.2018.09.024.

Franchi, L., Núñez, G., 2008. The Nlrp3 inflammasome is critical for aluminium hydroxide-mediated IL-1β secretion but dispensable for adjuvant activity. Eur. J. Immunol. 38, 2085–2089. https://doi.org/10.1002/eji.200838549.

Hoffmeyer, S., Burk, O., von Richter, O., Arnold, H.P., Brockmöller, J., Johne, A., et al., 2000. Functional polymorphisms of the human multidrug-resistance gene: multiple sequence variations and correlation of one allele with P-glycoprotein expression and activity in vivo. Proc. Natl. Acad. Sci. 97, 3473–3478. https://doi.org/10.1073/pnas.97.7.3473.

Hornung, V., Bauernfeind, F., Halle, A., Samstad, E.O., Kono, H., Rock, K.L., et al., 2008. Silica crystals and aluminum salts activate the NALP3 inflammasome through phagosomal destabilization. Nat. Immunol. 9, 847–856. https://doi.org/10.1038/ni.1631.

Jeong, C.H., Kwon, H.C., Cheng, W.N., Kim, D.H., Choi, Y., Han, S.G., 2020. Aluminum exposure promotes the metastatic proclivity of human colorectal cancer cells through matrix metalloproteinases and the TGF-β/Smad signaling pathway. Food Chem. Toxicol. 141, 111402. https://doi.org/10.1016/j.fct.2020.111402.

Jeong, C.H., Kwon, H.C., Kim, D.H., Cheng, W.N., Kang, S., Shin, D.-M., et al., 2020. Effects of aluminum on the integrity of the intestinal epithelium: an in vitro and in vivo study. Environ. Health Perspect. 128, 017013. https://doi.org/10.1289/EHP5701.

Kanneganti, T.-D., Ozören, N., Body-Malapel, M., Amer, A., Park, J.-H., Franchi, L., et al., 2006. Bacterial RNA and small antiviral compounds activate caspase-1 through cryopyrin/Nalp3. Nature 440, 233–236. https://doi.org/10.1038/nature04517.

Khan, Z., Combadière, C., Authier, F.-J., Itier, V., Lux, F., Exley, C., et al., 2013. Slow CCL2-dependent translocation of biopersistent particles from muscle to brain. BMC Med. 11, 99. https://doi.org/10.1186/1741-7015-11-99.

Khor, B., Gardet, A., Xavier, R.J., 2011. Genetics and pathogenesis of inflammatory bowel disease. Nature 474, 307–317. https://doi.org/10.1038/nature10209.

Kumar, A., Priyamvada, S., Ge, Y., Jayawardena, D., Singhal, M., Anbazhagan, A.N., et al., 2021. A novel role of SLC26A3 in the maintenance of intestinal epithelial barrier integrity. Gastroenterology 160, 1240–1255.e3. https://doi.org/10.1053/j.gastro.2020.11.008.

Kuroda, E., Ishii, K.J., Uematsu, S., Ohata, K., Coban, C., Akira, S., et al., 2011. Silica crystals and aluminum salts regulate the production of prostaglandin in macrophages via NALP3 inflammasome-independent mechanisms. Immunity 34, 514–526. https://doi.org/10.1016/j.immuni.2011.03.019.

Langmann, T., Schmitz, G., 2006. Loss of detoxification in inflammatory bowel disease. Nat. Clin. Pract. Gastroenterol. Hepatol. 3, 358–359. https://doi.org/10.1038/ncpgasthep0545.

Langmann, T., Moehle, C., Mauerer, R., Scharl, M., Liebisch, G., Zahn, A., et al., 2004. Loss of detoxification in inflammatory bowel disease: dysregulation of pregnane X receptor target genes. Gastroenterology 127, 26–40. https://doi.org/10.1053/j.gastro.2004.04.019.

Li, H., Willingham, S.B., Ting, J.P.-Y., Re, F., 2008. Cutting edge: inflammasome activation by alum and alum's adjuvant effect are mediated by NLRP3. J. Immunol. Baltim. Md. 1950 181, 17–21. https://doi.org/10.4049/jimmunol.181.1.17.

Li, J.-Y., Liu, J., Dong, D., Jia, X., McCouch, S.R., Kochian, L.V., 2014. Natural variation underlies alterations in nramp aluminum transporter (NRAT1) expression and function that play a key role in rice aluminum tolerance. Proc. Natl. Acad. Sci. 111, 6503–6508. https://doi.org/10.1073/pnas.1318975111.

McCloy, R.A., Rogers, S., Caldon, C.E., Lorca, T., Castro, A., Burgess, A., 2014. Partial inhibition of Cdk1 in G2 phase overrides the SAC and decouples mitotic events. Cell Cycle 13, 1400–1412. https://doi.org/10.4161/cc.28401.

McGovern, D.P.B., Kugathasan, S., Cho, J.H., 2015. Genetics of inflammatory bowel diseases. Gastroenterology 149, 1163–1176.e2. https://doi.org/10.1053/j.gastro.2015.08.001.

Molodecky, N.A., Soon, I.S., Rabi, D.M., Ghali, W.A., Ferris, M., Chernoff, G., et al., 2012. Increasing incidence and prevalence of the inflammatory bowel diseases with time, based on systematic review. Gastroenterology 142, 46–54.e42. https://doi.org/10.1053/j.gastro.2011.10.001.

Ng, S.C., 2014. Epidemiology of inflammatory bowel disease: focus on Asia. Best Pract. Res. Clin. Gastroenterol. 28, 363–372. https://doi.org/10.1016/j.bpg.2014.04.003.

Ng, S.C., Bernstein, C.N., Vatn, M.H., Lakatos, P.L., Loftus, E.V., Tysk, C., et al., 2013. Geographical variability and environmental risk factors in inflammatory bowel disease. Gut 62, 630–649. https://doi.org/10.1136/gutjnl-2012-303661.

Panwala, C.M., Jones, J.C., Viney, J.L., 1998. A novel model of inflammatory bowel disease: mice deficient for the multiple drug resistance gene, mdr1a, spontaneously develop colitis. J. Immunol. Baltim. Md. 1950 161, 5733–5744.

Pérez-Torras, S., Iglesias, I., Llopis, M., Lozano, J.J., Antolín, M., Guarner, F., et al., 2016. Transportome profiling identifies profound alterations in Crohn's disease partially restored by commensal bacteria. J. Crohns Colitis 10, 850–859. https://doi.org/10.1093/ecco-jcc/jjw042.

Pineton de Chambrun, G., Body-Malapel, M., Frey-Wagner, I., Djouina, M., Deknuydt, F., Atrott, K., et al., 2014. Aluminum enhances inflammation and decreases mucosal healing in experimental colitis in mice. Mucosal Immunol. 7, 589–601. https://doi.org/10.1038/mi.2013.78.

Potočnik, U., Ferkolj, I., Glavač, D., Dean, M., 2004. Polymorphisms in multidrug resistance 1 (MDR1) gene are associated with refractory Crohn disease and ulcerative colitis. Genes Immun. 5, 530–539. https://doi.org/10.1038/sj.gene.6364123.

Powell, J.J., Ainley, C.C., Evans, R., Thompson, R.P., 1994. Intestinal perfusion of dietary levels of aluminium: association with the mucosa. Gut 35, 1053–1057.

Qadir, M., O'Loughlin, K.L., Fricke, S.M., Williamson, N.A., Greco, W.R., Minderman, H., et al., 2005. Cyclosporin a is a broad-spectrum multidrug resistance modulator. Clin. Cancer Res. 11, 2320–2326. https://doi.org/10.1158/1078-0432.ccr-04-1725.

Rivas, M.A., Beaudoin, M., Gardet, A., Stevens, C., Sharma, Y., Zhang, C.K., et al., 2011. Deep resequencing of GWAS loci identifies independent rare variants associated with inflammatory bowel disease. Nat. Genet. 43, 1066–1073. https://doi.org/10.1038/ng.952.

Schindelin, J., Arganda-Carreras, I., Frise, E., Kaynig, V., Longair, M., Pietzsch, T., et al., 2012. Fiji - an open source platform for biological image analysis. Nat. Methods 9. https://doi.org/10.1038/nmeth.2019.

Shao, X., Lin, D., Sun, L., Wu, C., Yang, W., Jiang, Y., 2018. Association of ulcerative colitis with solute-linked carrier family 26 member A3 gene polymorphisms and its expression in colonic tissues in Chinese patients. Int. J. Color. Dis. 33, 1169–1172. https://doi.org/10.1007/s00384-018-3097-4.

Sirot, V., Traore, T., Guérin, T., Noël, L., Bachelot, M., Cravedi, J.-P., et al., 2018. French infant total diet study: exposure to selected trace elements and associated health risks. Food Chem. Toxicol. 120, 625–633. https://doi.org/10.1016/j.fct.2018.07.062.

Staley, E.M., Schoeb, T.R., Lorenz, R.G., 2009. Differential susceptibility of P-glycoprotein deficient mice to colitis induction by environmental insults. Inflamm. Bowel Dis. 15, 684–696. https://doi.org/10.1002/ibd.20824.

Tanner, S.M., Staley, E.M., Lorenz, R.G., 2013. Altered generation of induced regulatory T cells in the FVB.mdr1a−/− mouse model of colitis. Mucosal Immunol. 6, 309–323. https://doi.org/10.1038/mi.2012.73.

Torres, J., Mehandru, S., Colombel, J.-F., Peyrin-Biroulet, L., 2017. Crohn's disease. Lancet Lond. Engl. 389, 1741–1755. https://doi.org/10.1016/S0140-6736(16)31711-1.

Ungaro, R., Mehandru, S., Allen, P.B., Peyrin-Biroulet, L., Colombel, J.-F., 2017. Ulcerative colitis. Lancet 389, 1756–1770. https://doi.org/10.1016/S0140-6736(16)32126-2.

VanDuyn, N., Settivari, R., LeVora, J., Zhou, S., Unrine, J., Nass, R., 2013. The metal transporter SMF-3/DMT-1 mediates aluminum-induced dopamine neuron degeneration. J. Neurochem. 124, 147–157. https://doi.org/10.1111/jnc.12072.

Vedamurthy, A., Ananthakrishnan, A.N., 2019. Influence of environmental factors in the development and outcomes of inflammatory bowel disease. Gastroenterol. Hepatol. 15, 72–82.

Vignal, C., Desreumaux, P., Body-Malapel, M., 2016. Gut: an underestimated target organ for aluminum. Morphol. Bull. Assoc. Anat. 100, 75–84. https://doi.org/10.1016/j.morpho.2016.01.003.

Wang, Y., Liu, M., Zhang, J., Liu, Y., Kopp, M., Zheng, W., et al., 2018. Multidrug resistance protein 1 deficiency promotes doxorubicin-induced ovarian toxicity in female mice. Toxicol. Sci. 163, 279–292. https://doi.org/10.1093/toxsci/kfy038.

Weersma, R.K., Van Dullemen, H.M., Van Der Steege, G., Nolte, I.M., Kleibeuker, J.H., Dijkstra, G., 2007. Review article: inflammatory bowel disease and genetics. Aliment. Pharmacol. Ther. 26, 57–65. https://doi.org/10.1111/j.1365-2036.2007.03476.x.

Yokel, R.A., Florence, R.L., 2008. Aluminum bioavailability from tea infusion. Food Chem. Toxicol. 46, 3659–3663. https://doi.org/10.1016/j.fct.2008.09.041.